



Improvement of the Fatigue Resistance and Increase Its Life of Specimens of Naval Brass Alloy Using Laser Shock Wave Processing

R.S. Jawad¹, A. Kadhim^{2,*}, S.M. Fayadh³, T.K. Abed⁴

¹Energy and Renewable Energies Technology Centre, University of Technology, Baghdad – 10001, Iraq.

²Laser & Optoelectronics Engineering Department, University of Technology (UOT), Baghdad – 10001, Iraq.

³Ministry of Education, Anbar – 31001, Iraq.

⁴Environmental Research Center, University of Technology (UOT), Baghdad – 10001, Iraq.

ARTICLE DETAILS

Article history:

Received 11 December 2015

Accepted 26 January 2016

Available online 03 February 2016

Keywords:

Fatigue Life
Naval Brass Alloy
Laser Shock Process

ABSTRACT

Laser shock processing (LSP) was performed on naval brass alloy specimen to reveal effectiveness on fatigue life. LSP experimental array was performed as follows: A convergent lens was used to deliver 0.5-1 J/pulse (1064 nm). In a 10 ns, laser FWHM pulse produced by Q-switched Nd:YAG laser of 6 Hz with spots of 0.5-2 mm in diameter moving forward along the work piece with pulse density of 500 pulses/cm². Deionized water (3 mm thickness) was used as a transparent confining layer while the non-prate black paint (20 μm thickness) was used as an absorbing layer of laser beam. The optimum values of 1mm spot size, pulse energy of 1 J. LSP effective parameters, microstructure and fatigue life test were evaluated. Chemical composition analysis was conducted. The microstructure analysis included surface morphology by SEM, grain analysis by AFM. The results demonstrated that the LSP can be improving fatigue resistance for specimens which were used in this work by comparing with the untreated specimens. The fatigue life's of the specimens after LSP was obviously increased by 64% at lower stress level due to the compressive residual stresses near the surface.

1. Introduction

Among the wide variety of surface treatments investigated for improving properties of materials, laser shock surface treatments was developed about 25 years ago in the USA with particular application to enhance some mechanical properties [1]. More recently, surface treatment technologies had become more and more important in industry in order to cut costs and avoid the need for expensive materials [2]. Laser materials processing could mainly be carried out by three methods; without melting such as (transformation hardening, bending and magnetic domain control which required low power density), melting (surface melting, glazing, cladding, welding and cutting which required high power density), while the third way was by vaporization (cutting, drilling, ablation which require substantially high power density within a very short interaction pulse time) [3, 4]. One of the major advantages of the laser materials processing was the possibility of accurate control of the area where laser radiation should be delivered, as well as the amount and rate of energy deposition since laser beams could be easily directed to fatigue-critical areas without masking [5]. In the field of surface treatments, with the advent of high-power lasers, laser shock processing (LSP) had emerged as a new and very promising technique to increase the resistance of metals and alloys to fatigue, wear and corrosion [6, 7]. Unlike other laser applications, LSP was not a thermal rather a mechanical process for treating materials [8]. It involved a high-energy laser beam combined with suitable overlays to generate mechanical pressure waves of up to 6–10 GPa on the surface of a metal [9]. Once the peak pressure exceeded material yield strength, the transient shock pressure was caused severe plastic deformation, refined grain size, compressive residual stresses, and increased hardness at the surface and in the subsurface. As a result, the mechanical properties on the surface were enhanced [10, 11]. The commonly recognized aspects of laser-solid interaction could be generalized as follows: laser-solid interaction, removal of sample particles, and plasma formation and expansion. The energy of a pulsed or continuous wave laser incident beam on surface of solid target caused rapid heating by absorption operation.

The photons of the incident laser beam promoted electrons with metal to a higher energy state, and the heating occurred when excited electrons lost energy to return to an equilibrium state, so were scattered by lattice defects like usual non-crystalline regions in a crystal such as dislocations and grain boundaries. In this case, the overall effect is to convert electronic energy derived from the beam of incident photons into heat [4, 12, 13]. This radiation will, in many cases, would be absorbed by the plume, leading to an attenuation of the light intensity incident on the target and excitation and ionization of species in the plume and due to the high temperature, the plasma finally was formed in material plume and subsequent optical emission would result [14]. In particular, ionization occurred due to two simultaneous mechanisms: the absorption of multiple photons and the ionization by the electron impact (avalanche ionization). The relative contribution of both mechanisms depended on laser wavelength, pulse duration, intensity and the atomic number of the sample [15]. One of major advantages of the laser as a tool for material processing was the ability to be precisely controlled which exercised through the proper selection of laser processing parameters to achieve the desired material modification [12]. Once the high power laser energy deposited on a metallic target surface it would be absorbed by free electrons, and then transferred to the lattice, which led to electron-lattice coupling. Ablation was initiated with melting, dissociation, and vaporization of materials. At a laser intensity of about 10³ W/cm², the local temperature approached the boiling point of the material. Material removal was controlled by thermal conduction, and at approximately 10⁷–10¹⁰ W/cm² (depending on laser wavelength and pulse duration) the vapor plume would expand and be partially ionized. After the phase transition, as a result opaque plasma is formed with a duration of several picoseconds. This plasma was contained electrons, ions, neutral species, as well as excited species from the solid target [4, 14]. The most important difference between laser produced plasma of solids in vacuum or diluted gas and in liquids is the confinement movement of the plasma plume by liquids environment. Therefore, a series of processes, including generation, transformation, and condensation of the produced plasma, would take place under the condition of the liquid confinement. Importantly, the confinement from liquids could greatly influenced the thermodynamic and kinetic properties of the evolution of the plasma plume, and further cause distinctly the different environments of the condensing phase formation

*Corresponding Author

Email Address: abdulhadikadhimi5@gmail.com (Abdilhadi Kadhimi)

from that of laser ablation of solids in vacuum or diluted gas. Therefore, the understanding of fundamental aspects of the evolution of the plasma plume from laser ablation of solids in liquids was essential to find important potential in technology such as materials processing [16]. The laser produced plasma of solids in liquid environments involved focusing a high power laser beam onto the surface of a solid target, which was submerged beneath a transparent liquid for laser beam wavelength (such as water). The initial process was the interaction of the laser with the target which caused instantaneous vaporization of the target surface and a small amount of surrounding liquid, due to absorption of laser beam energy in the form of an ablation plume, which contains species such as atoms, ions, and clusters, travelled with high kinetic energy [17, 18]. Furthermore, the plasma-induced pressure would lead to an increase in the additional temperature of the laser-induced plasma. Therefore, the shock wave generated by the expansion of the laser-induced plasma under the confinement of liquid pushed the laser-induced plasma into a thermodynamic state of the higher temperature, higher pressure, higher density and confined to smaller volume than that of the initially generated plasma by creating the additional pressure and temperature increases in the laser-induced plasma [19, 18].

Four kinds of chemical reactions would take place in the laser-induced plasma and the interface between the liquid and the laser-induced plasma during the transformation of the laser-induced plasma, respectively. They were:

1. Chemical reaction occurred inside the laser-induced plasma and could be formed by the high temperature chemical reactions between the ablations from the target [20].
2. Chemical reaction took place inside the laser-induced plasma, here, the reactant species were from the target and the liquid [21, 18].
3. A set of chemical reactions occurred at the interface between the laser-induced plasma and the liquid, because the thermodynamic state with high temperature, high pressure and high density of the laser-induced plasma provided a good opportunity for the high-temperature chemical reactions between the ablated species from the target and the molecules of the liquid [18].
4. Chemical reaction occurred inside the liquid. The extremely high pressure in front of the laser-induced plasma would impinge the ablation species from the solid target at the plasma-liquid interface into the liquid [16, 18].

Many materials displayed pronounced improvements in fatigue life with laser shock processing [21]. The beneficial effects of laser shock processing may originated from surface compressive stresses in the large affected depth and surface quality, which delayed the development of fatigue cracking [22]. LSP served to enhance fatigue properties by improving the resistance against fatigue crack initiation and propagation [23, 24]. The crack propagation rate was slowed considerably by this behavior, and fatigue life was significantly increased, the crack itself is not easily detected. This was sometimes a concern in failure-sensitive applications [18, 21]. Investigations into several different aspects of the fatigue behaviors, such as fatigue life and fatigue strength, had been reported. The effects of laser shocking on fatigue properties had been investigated for aluminum alloys, steels and titanium alloys and had shown that LSP can increase fatigue strength and fatigue life [22]. The phenomenon might be attributed either to the submission of the irradiated surface to an elasto-plastic wave generating uniaxial plastic strain or to the relatively low surface roughness of the specimen. Since the high surface roughness might induced numerous stress concentrations, the low fatigue lives of the untreated specimen might be due to the high surface roughness [2, 25, 26]. In continuous to or work [27-32], herein we try to improving the fatigue life of brass alloy. Comparing with the fatigue life of the sample untreated by LSP, fatigue life is increased by 64% for brass at lower stress level. The fatigue crack initiation and growth of the sample treated by LSP could be restrained more effectively.

2. Experimental Methods

2.1 Samples Preparation

The samples were manufactured from Naval brass ASTM B21. They were cut into a rectangular shape with dimensions of 70×10×30 mm³. The chemical composition and the mechanical properties of the brass alloy were shown in Tables 1 and 2 respectively. Prior to the laser shock, the samples were polished with SiC paper to different grades of roughness ranging from 400#, 600#, 800#, 1200#, 1600# to 2000# and then polished by diamond best with lubricated liquid on cloth paper, followed by washing in deionized water while ethanol was used to degrease the sample surface in order to be used in LSP experiments.

Table 1 Chemical composition of brass alloy

Composition	Zn	Pb	Sn	P	Fe	Ni	Si	Sb	Co	Al	Cu
Per. (wt.%)	40.2	0.06	0.15	0.007	0.04	0.14	0.001	0.007	0.002	0.02	Bal.

Table 2 The mechanical properties of brass alloy

Yield limit (MPa)	Ultimate tensile strength (N/mm ²)	Elastic modulus (MPa)	Elongation (%)	Micro-hardness (Hv)
273	400	149800	12.8	122

2.2 LSP Experimental Array

During LSP, the shock waves were induced by a Q-switched Nd-YAG repetition-rate laser with a wavelength of 1064 nm, a pulse duration about 10 ns at FWHM, a spot size varied from 0.5 mm to 2 mm by focusing lens of focal length 12 cm, and the laser energy was varied from 500 mJ to 1J. The pulse energy of a Q-switched Nd-YAG laser measured by a Genetic QE12SP-S-MT joule meter as. He-Ne laser ($\lambda=632.8$ nm) was used for optical alignment purpose. The environment water was filtered, de-ionized; the target was covered with water layer thicknesses of 3mm was used as the transparent confining layer and the non-prate black paint with a thickness of 20 μ m was used as an absorbing layer and to protect the sample surface from thermal effect. The thickness of coating layer was measured by digital thickness meter. During LSP impact, the laser beam was perpendicular to the sample surface and the water layer was replaced after each line impact to maintain the water purity. The overlapping rate was 50% between two adjacent spots in order to ensure no blind area at the LSP shocked region and the pulse density was 500 pulse/cm². LSP experimental array as shown in the Fig. 1.

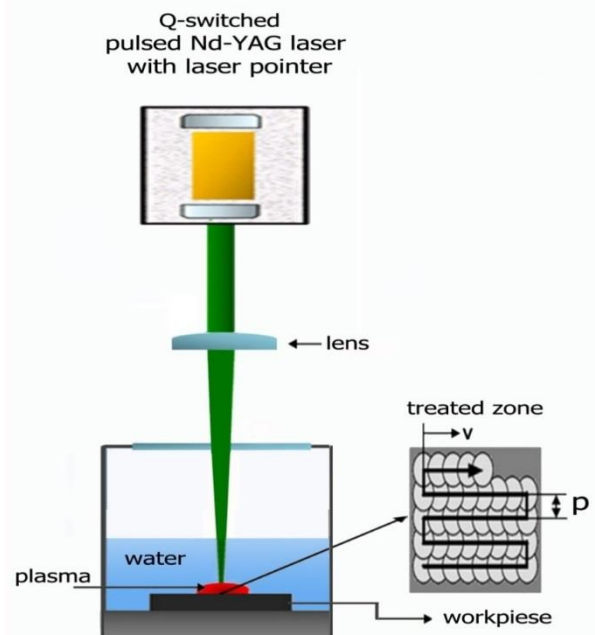


Fig. 1 Schematic diagram of the experimental setup for laser shock processing and the irradiation pattern on a sample

2.3 Fatigue Test

The specimens were prepared for fatigue test by cutting them into rectangular shapes with dimensions of 70×10×30 mm³. Alternating bending fatigue machine was used (Hi-Tech company England) to test all prepared specimens. High speeds were possible, so millions of cycles could be achieved within hours. The following equation (3-2) was used to calculate the applied stress on the specimens

$$\sigma = \frac{1.5Et\delta^2}{l^2}$$

where, σ : applied stress, E: elastic modulus of the material, t : the thickness of used sample, δ : free end deflection, and l : the length of cantilever after applied of stress. By variation of the sample length under the stress and the deflection value it was possible to identify levels of stress, it must be less than yield stress of material. The number of cycles to failure was identified after run the alternating bending fatigue machine.

3. Results and Discussion

3.1 Fatigue Resistance and Fatigue Life

All samples were subjected to the fatigue test have treated under conditions, spot size of 1mm, pulse energy of 1 J and water layer thickness of 3 mm.

The S-N curves for specimens of untreated LSP and treated LSP were shown in Fig. 2. The results revealed that, the fatigue lives of treated and untreated LSP at different applied stress levels. It is clear that the fatigue life of the treated specimen was obviously higher than that of the untreated specimens at the same applied stress. By comparing with untreated LSP samples specimens for lowest stress in the test, the fatigue life increased by 64% at 149 MPa stress for brass. According to these results, the LSP has improved the fatigue life of the brass. The improvement was due to deeply compressive residual stress generated in metal surface by LSP and heavily deformed surface layer. The material below the irradiated surface is submitted to an elasto-plastic wave generating uniaxial plastic strain. The surrounding material is opposed to that strain and therefore induced, after the interaction, biaxial compressive residual stresses. The compressive residual stresses with the values of several hundred MPa will be generated near the specimen surface after LSP. It is well known that as fatigue cracks mostly originate at the surface of materials, the fatigue behavior of mechanical parts depends strongly on their mechanical surface states, and a compressive surface layer prevents crack opening and growth and therefore has a beneficial effect on the fatigue performance.

Experimental results showed that the compressive stress at the surface would inhibit the crack initiation and growth during the LCF testing. Hence, the compressive stresses at the surface may had an obvious attribution to the improvement of the fatigue performance of the specimen after LSP.

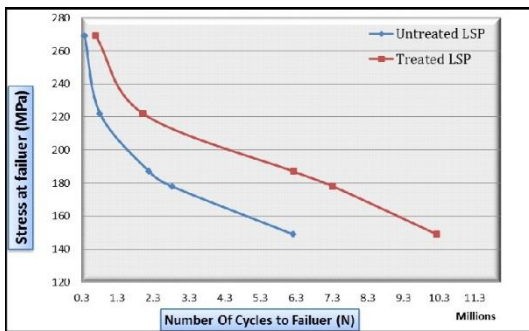


Fig. 2 S-N curves of brass samples; treated and untreated LSP samples at different applied stress levels

3.2 SEM of Fatigue Crack Area

Scanning Electron Microscope (SEM) type (FESEM, SUPRA TM 55vp Zeiss, England product) was used to analyze surface morphology of all specimens before and after LSP treatment and all mechanical tests. The measurements were conducted in UKM Malaysia University.

Fig. 3, shows Scanning Electron Microscopy micrographs of surface for naval brass alloy. SEM micrograph before the laser treatment show that the alloy before laser treatment had a homogeneous surface. SEM micrograph of the treated surface proved that the LSP caused an ablation and melting of thin surface layer of the treated alloy. The rapid heating and melting accompanied by a high pressure of plasma cause the liquid metal to spill from the central part of the treated area towards the periphery, due to cooling. The melted features most observed on the surface after LSP were craters, holes, solidified droplets, splash-like spills and molten flowing layers. It was found that the central part of the treated area free of cracks. Finally, the SEM investigations indicate that the process of the laser shock processing is not purely mechanical, it has some thermal effects at the metal surface.

Fig. 3a and b showed the SEM micrograph of fatigue crack areas of untreated and treated LSP samples for brass alloy. From these micrographs, it was found that the crack origin of the untreated samples occurs at the material surface was little bigger than that of treated LSP samples. The fatigue crack growth presented the sectorial radial shape and the ridge was clear with layered distribution.

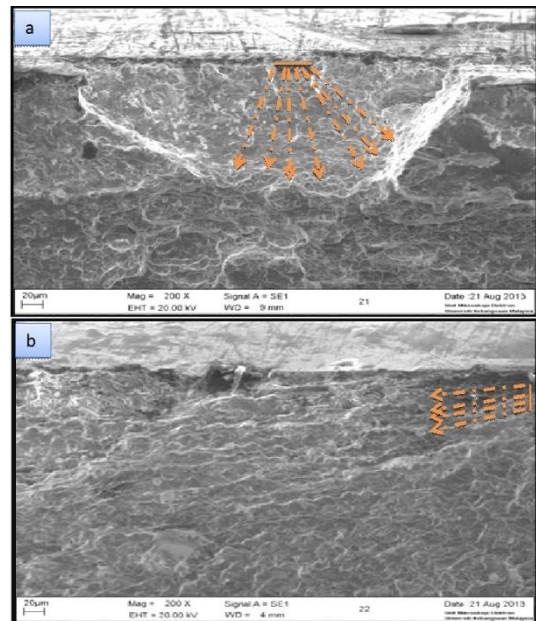


Fig. 3 SEM micrographs of fatigue crack areas of brass samples a) untreated LSP and b) treated LSP.

Compared to the untreated LSP samples, the range and the radian of the main crack propagation for treated LSP samples were a little smaller. It could be concluded that more time of the crack initiation of LSP treated samples was needed than that of untreated LSP samples. The total stress on the surface layer was much less than the fatigue limit of the strengthening layer and that may due to the compressive residual stress generated by LSP and its strengthening effect and its lead to reduce the peak value of tensile stress at the stress concentration part such as sharp-angled place.

3.3 AFM

Atomic Force Microscope (AFM) type (AA3000 Scanning Probe Microscope SPM, tip NSC35/AIBS) from Angstrom Ad-Vance Inc.

Fig. 4a and b show the AFM images of grains analysis for the surface layers of the untreated and the treated LSP samples for naval brass alloy. It can be distinctly observed that the average size of the original grain in the surface layer of the untreated sample is larger than that of LSP treated sample. The average grain size has decreased from 0.255 μm before LSP to 0.174 μm after LSP. The refinement of grain size in the near-surface region is due to dislocation movement and dispersion strengthening of LSP process. The reaction between laser shock wave and the metal target will be generated near the target surface after LSP, leading to the increment of the dislocation density and the microstructural deformation near the surface. LSP caused plastic deformation of the specimen surface which was recessed by several microns due to the plastic deformation, and high density dislocations.

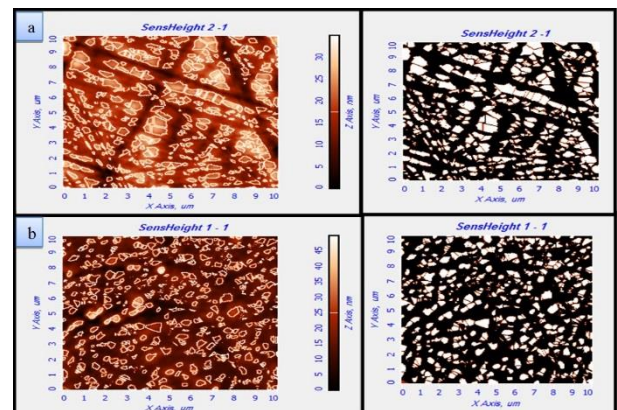


Fig. 4 AFM images of grains analysis in surface layer of naval brass alloy a) the untreated LSP sample and b) treated LSP sample

4. Conclusion

The fatigue test results showed that LSP is an effective surface treatment technique for improving the fatigue life of brass alloy. Comparing with the fatigue life of the sample untreated by LSP, fatigue life is increased by 64% for brass at lower stress level. The fatigue crack initiation and growth of the sample treated by LSP could be restrained more effectively.

References

- [1] P. Peyre, L. Berthe, X. Scherpereel, R. Fabbro, Laser-shock processing of aluminum-coated 55C1 steel in water-confinement regime, characterization and application to high-cycle fatigue behavior, *J. Mater. Sci.* 33 (1998) 1421-1429.
- [2] I.B. Roman, A.S. Banea, M.H. Tîereani, A review on mechanical properties of metallic materials after laser shock processing, *Eng. Sci.* 4 (2011) 81-86.
- [3] J. Kusinski, S. Kac, A. Kopia, A. Radziszewska, M. Rozmusgornikowska, B. Major, et al, Laser modification of the materials surface layer – a review paper, *Tech. Sci.* 60 (2012) 711-728.
- [4] T.H. Maiman, Stimulated optical emission in ruby, *Nature* 187 (1960) 493-494.
- [5] K. Sasaki, N. Takada, Liquid-phase laser ablation, *Pure Appl. Chem.* 82 (2010) 1317-1327.
- [6] C. Rubio-Gonzalez, C. Felix-Martinez, G. Gomez-Rosas, J.L. Ocanac, M. Morales, J.A. Porro, Effect of laser shock processing on fatigue crack growth of duplex stainless steel, *Mater. Sci. Eng. A* 528 (2011) 914-919.
- [7] Y. Zhang, J. Lu, K. Luo, Surface integrity of LY2 Al alloy subjected to laser shock processing, *Springer Series Mater. Sci. Berlin Heidelberg*, 2013.
- [8] U. Trdan, J. Ocaña, J. Grum, Surface modification of aluminium alloys with laser shock processing, *J. Mech. Eng.* 57 (2011) 385-393.
- [9] H. Allan Clauer, Laser shock peening for fatigue resistance, TMS, Warrendale, PA., 1996, pp.217-230.
- [10] A.F.M. Arif, Numerical prediction of plastic deformation and residual stresses induced by laser shock processing, *J. Mater. Process. Technol.* 136 (2003) 120-138.
- [11] Y.B. Guo, Laser shock peening: modeling, simulations, and applications, Department Mechanical Engineering, The University of Alabama, USA, 2011, pp.332-357.
- [12] L. Zhanga, K.Y. Luoa, J.Z. Lua, Y.K. Zhanga, F.Z. Daia, J.W. Zhonga, Effects of laser shock processing with different shocked paths on mechanical properties of laser welded ANSI 304 stainless steel joint, *Mater. Sci. Eng. A* 528 (2011) 4652-4657.
- [13] S. Matthew, B. Craig, Fundamentals of laser – material interaction and application to multiscale surface modification, Princeton University, USA, 2009.
- [14] M. Frederik, C. Claeysens, G. Fuge, S. Henley, Pulsed laser ablation and deposition of thin films, *Chem. Soc. Rev.* 33 (2004) 23-31.
- [15] J. Dutta, I. Manna, Laser processing of materials, *Sadhana* 28 (2003) 495-562.
- [16] B. Annemie, C. Zhaoyang, Effect of laser parameters on laser ablation and laser-induced plasma formation: A numerical modeling investigation, *Spectrochim. Acta B* 60 (2005) 1280-1307.
- [17] D. Bigoni, M. Milani, R. Jafer, C. Liberatore, S. Tarazi, L. Antonelli, D. Batani Influence of mechanical and thermal material properties on laser-produced crater-morphology and their study by focused ion beam & scanning electron microscope imaging, *J. Laser Micro/Nanoeng.* 5 (2010) 1-2.
- [18] G.W. Yang, Laser ablation in liquid: application in the synthesis of nanocrystals, *Mater. Sci.* 52 (2007) 648-698.
- [19] C.A. Askar, E.M. Moroz, Pressure on evaporation of matter in a radiation beam, *J. Experiment. Theoretical Phys. Lett.* 16 (1963) 1638-1644.
- [20] S. Matthew, B. Craig, Liquid-phase pulsed laser ablation, Springer, Verlag Berlin Heidelberg, 2010.
- [21] B. Kumar, R. Tharejaa, Synthesis of nanoparticles in laser ablation of aluminum in liquid, *J. Appl. Phys.* 108 (2010) 064906.
- [22] A.H. Clauer, C.T. Ford, S.C. Ford, The effects of laser shock processing on the fatigue properties of T-3 aluminum, In: *Lasers in materials processing*, American Society for Metals, USA, 1983.
- [23] L. Zhang, J.Z. Lu, Y.K. hang, K.Y. Luo, J.W. Zhong, C.Y. Cui, et al, Effects of different shocked paths on fatigue property of 7050-T7451 aluminum alloy during two-sided laser shock processing, *Mater. Design* 32 (2011) 480-486.
- [24] X.D. Ren, D.W. Jiang, Y.K. Zhang, T. Zhang, H.B. Guan, X.M. Qian, Effects of laser shock processing on 00Cr12 mechanical properties in the temperature range from 25 °C to 600 °C, *Appl. Surf. Sci.* 257 (2010) 1712-1715.
- [25] S. Charles, W. Tao, Y. Lin, Cl. Graham, M. Yiu-Wing, Laser shock processing and its effects on microstructure and properties of metal alloys, *Int. J. Fatigue* 24 (2002) 1021-1036.
- [26] X.D. Ren, T. Zhang, Y.K. Zhang, D.W. Jiang, H.F. Yongzhuo, H.B. Guan, X.M. Qian, Mechanical properties and residual stresses changing on 00Cr12 alloy by nanoseconds laser shock processing at high temperatures, *Mater. Sci. Eng. A* 528 (2011) 1949-1953.
- [27] H. Hussein, A. Kadhim, A. Al-Amiery, A. Kadhum, A. Mohamad, Enhancement of the wear resistance and microhardness of aluminum alloy by Nd: YAG laser treatment, *Scientific World Jour.* 2014 (2014) 842062.
- [28] Kadhim, Salim, E. Fayadh, S. Al-Amiery, A. Kadhum, A. Mohamad, Effect of multipath laser shock processing on microhardness, surface roughness, and wear resistance of 2024-t3 Al alloy, *Scientific World Jour.* 2014 (2014) 490951.
- [29] E. Yousif, A. Al-Amiery, A. Kadhim, A. Kadhum, A. Mohamad, Photostabilizing efficiency of PVC in the presence of schiff bases as photostabilizers, *Molecules* 20 (2015) 19886-19899.
- [30] S. Junaedi, A. Al-Amiery, A. Kadhim, A. Kadhum, A. Mohamad, Inhibition effects of a synthesized novel 4-aminoantipyrine derivative on the corrosion of mild steel in hydrochloric acid solution together with quantum chemical studies, *Int. J. Mol. Sci.* 14 (2013) 11915-11928.
- [31] A. Alobaidy, A. Kadhum, S. Al-Baghdadi, A. Al-Amiery, A. Kadhum E. Yousif, A. Mohamad, Eco-friendly corrosion inhibitor: experimental studies on the corrosion inhibition performance of creatinine for mild steel in HCl complemented with quantum chemical calculations, *Int. J. Electrochem. Sci.* 10 (2015) 3961 – 3972.
- [32] A. Al-Amiery, A. Kadhum, A. Kadhim, A. Mohamad, C. How, S. Junaedi, Inhibition of mild steel corrosion in sulfuric acid solution by new schiff base, *Materials* 7 (2014) 787-804.